Creating a New, Smarter Health Care

The Highlights Lecture is presented at the closing session of each SNM Annual Meeting by Henry N. Wagner, Jr., MD. This year's lecture was presented on June 17 in Toronto, Canada. Frederic Fahey, DSc, chair of the Scientific Committee, introduced Dr. Wagner. Note that items in brackets represent abstract numbers from The Journal of Nuclear Medicine *(2009;50[suppl2]).*

This marks the 50th consecutive SNM Annual Meeting that I have attended, and I can attest that from 1959 to the present the meeting has gotten better every time. No one could have conceived in those early days of the range and extent of development to come in nuclear medicine and allied techniques. Today's lecture also marks my 33rd consecutive Highlights Lecture. As I have noted in previous lectures, attending this meeting—with its hundreds and hundreds of scientific and educational presentations and posters—is like taking a drink of water from a fire hose. My role is to turn down the flow. I want to extend my thanks to all of you who have helped in this effort this year.

More than half of the presentations at this meeting came from outside the United States. Table 1 shows that 733 presentations (44.7% of the total) were from the United States, with large numbers of papers from other countries. Japan, Germany, and Korea together accounted for another 24.1%.

If we look back at the subject matter of presentations at this meeting over the years, we see a period from the early 1980s to the mid-1990s during which the numbers of PET and SPECT presentations ran more or less parallel (Fig. 1). But beginning about 10 y ago, PET and PET/CT began to take off, with annual numbers of papers rising rapidly while SPECT and SPECT/CT plateaued. This year we saw 978 (59.6% of total) presentations focused on either PET or PET/CT and 290 (17.7%) on SPECT and SPECT/CT.

We also saw PET/MR imaging on the rise, with 38 presentations. Bindseil et al. [1530] from the University of Western Ontario (London, Canada) reported on "Hybrid images from a combined PET and field-cycled MRI system." The challenge in the development of PET/MR imaging is to ensure that the 2 systems do not interfere with each other. These researchers developed a field-cycled MR imaging system that uses novel T1 contrast and offers advantages over conventional MR imaging (Fig. 2). Among these advantages are significant reductions in artifacts, enabling imaging around metallic implants. The PET portion of the apparatus can be used when the magnetic fields are off.

Herzog et al. [1539] from the Forschungszentrum Jülich (Germany) and Siemens Medical Solutions (Knoxville, TN) reported on the "Performance of the 3T MR-BrainPET," which simultaneously records MR and ^{18}F-FDG PET images. In the upper row of Figure 3, T1-weighted images were obtained 10 min after injection of the ^{18}F-FDG. The middle row images were obtained 20–50 min after injection. The combined fusion of the images is shown in the third row. The authors noted that these promising results will be expanded with National Electrical Manufacturers Association–guided tests. The very high quality seen in these images is representative of many that were shown at this meeting.

Henry N. Wagner, Jr., MD

Creating Smarter Health Care

Each year, I pick what I call the Highlights theme of the meeting. For SNM 2009 that theme is "Creating a New Smarter Health Care." John Calvin said 4 centuries ago that, "Where there is no vision, the people perish." Today we can say, "Where there is no molecular imaging, the patients perish." The challenges that we face as we look ahead are many. First, the costs of health care in the United States, now $2.5 trillion/y, must be addressed. Technology is becoming increasingly complex and costly. Physicians, other health care providers, chemists, and technologists are in short supply. More than ever before, we need to show the public and our political leaders the key role that molecular medicine can play in containing costs and improving care.

We must be involved today not only in basic and clinical science but also in the economics and politics of health care. We must examine and publish cost and effectiveness data as well as data about the clinical value of molecular medicine. We must apply for and receive funds from the growing number of governmental comparative effectiveness research programs, which have been budgeted at $1.5 billion by the current administration.

We must also educate the public about what I call the "molecular theory of disease." Information is carried throughout our bodies in the form of molecular messages that define body structures and functions, provide intra- and intercellular communication, and determine the response to stress. Disease results when receptor molecules on or within cells do not receive the right messages or the cells fail to respond to such messages. No medical specialty is better equipped to transfer basic science to the care of patients and the prevention of disease than molecular medicine. Comparative effectiveness research, which is now being encouraged and will develop at an accelerating rate, provides us with

TABLE 1. SNM 2009 Annual Meeting Presentations by Country*

United States	733	44.7%
Japan	148	9.0%
Germany	131	8.0%
Korea	116	7.1%
China	77	4.7%
Canada	73	4.5%
France	70	4.3%
United Kingdom	58	3.5%
Italy	49	3.0%
Australia	44	2.7%
Netherlands	43	2.6%
India	41	2.5%

*The 12 countries with the highest numbers of presentations are included in this table.

enormous opportunities to advance the promise of molecular medicine.

We must also show the cost effectiveness of knowledge. Increasing knowledge is expensive, but making correct decisions decreases the cost of caring for each individual patient, thereby making it possible to increase productivity. Decreased cost and improved patient care will result in a dramatic increase in demand for molecular imaging.

The essence of molecular imaging hinges on a mechanistic transfer of vital messages. These messages, in the form of molecules, circulate around the body until they bump, fit, and stick into specific receptors to bring about a specific action. The message is carried in time and space. Figure 4 is an artist's rendering of what could be an antigen, drug, or neurotransmitter finding a specific site on a molecule, where it sticks, fits, and brings about action. This is an image I have shown before and will show again. It captures the basic process that underlies the success of molecular imaging.

Three disciplines can be woven together to create smarter health care: genetics, pharmacology, and molecular

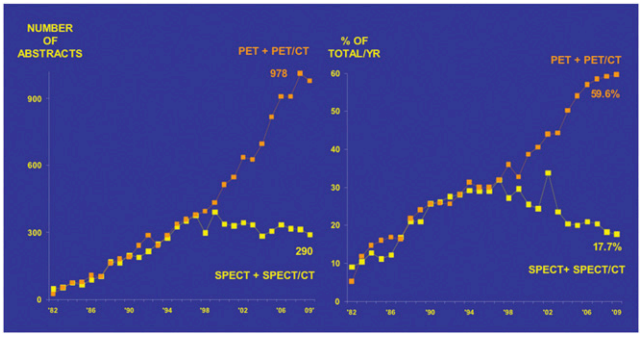

FIGURE 1. Left, number of PET and SPECT presentations at SNM annual meetings, 1982–2009. Right, PET and SPECT presentations as percentages of total presentations at each meeting, 1982–2009.

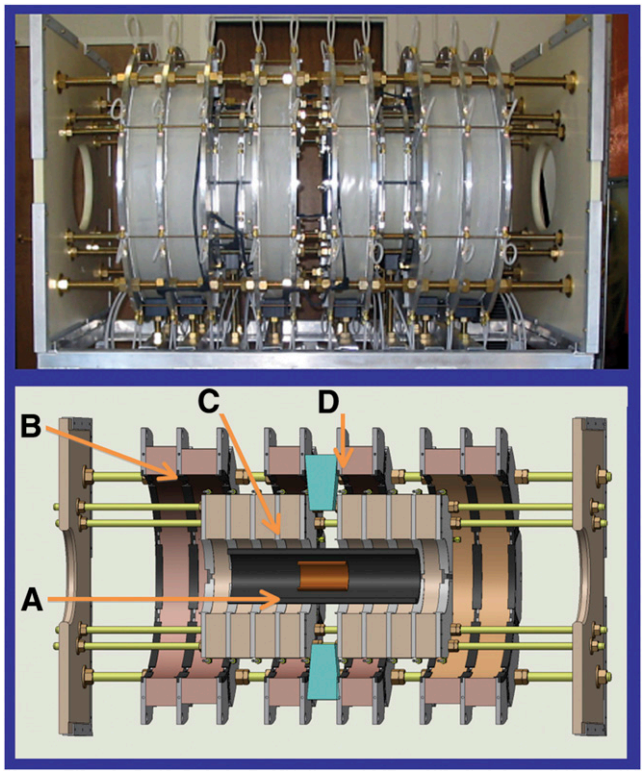

FIGURE 2. Top, combined PET and field-cycled MR imaging unit. Bottom, cutaway diagram of device: (A) gradients, shims, and radiofrequency coil; (B) readout magnet; (C) polarizing magnet; (D) PET, 2 detectors.

imaging. Tens of thousands or even millions of different molecular processes occur in the human body, and each is a potential target. The number of potentially useful tracers that can be developed to address these targets and improve treatment and care is almost limitless.

Shenoy et al. [1002] from the National Heart, Lung, and Blood Institute (Bethesda, MD) described "Ongoing production of diverse molecular imaging probes." (I prefer to use the term tracers rather than probes, because probes have been used traditionally in nuclear medicine to denote simple devices that make measurements, not the chemicals themselves.) These researchers are part of the Imaging Probe Development Center, initiated as part of the National Institutes of Health (NIH) Roadmap for Medical Research, created by a radiologist, Elias Zerhouni, MD, during his tenure as NIH director. The center provides a resource for the entire NIH community by producing and developing tracers that would otherwise be difficult to obtain. The center has active collaborations with 15 of the 27 NIH institutes and centers, which represent molecular imaging interests across a broad range of diseases. Studies currently being carried out there include investigations of ^{125}I-adenosine analogs, ^{124}I- and ^{125}I-thyroxine analogs, ^{3}H- and ^{125}H-vasopressin analogs, ^{18}F-FHBG, ^{68}Ga-DOTA-affibodies, and ^{111}In antibodies.

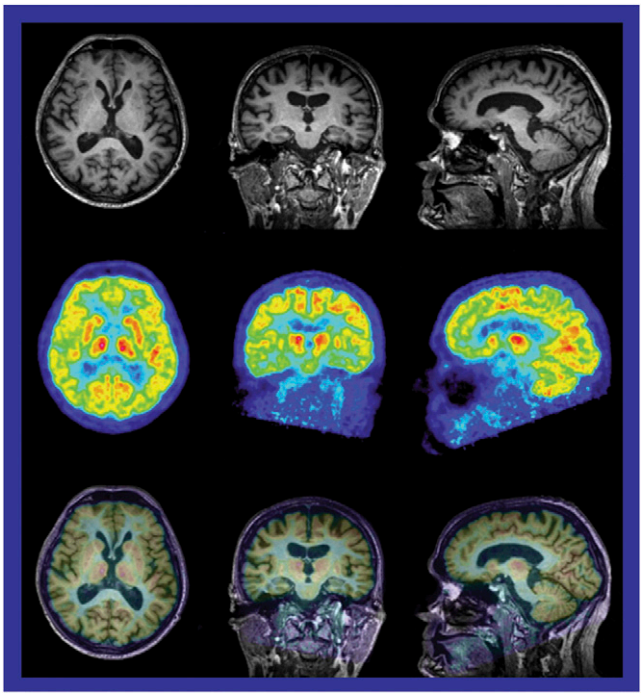

FIGURE 3. Simultaneously recorded MR/PET images. Top row, T1-weighted MR images acquired 10 min after injection of ^{18}F-FDG; middle row, PET images acquired 20–50 minutes after tracer injection; bottom row, combined MR/PET images.

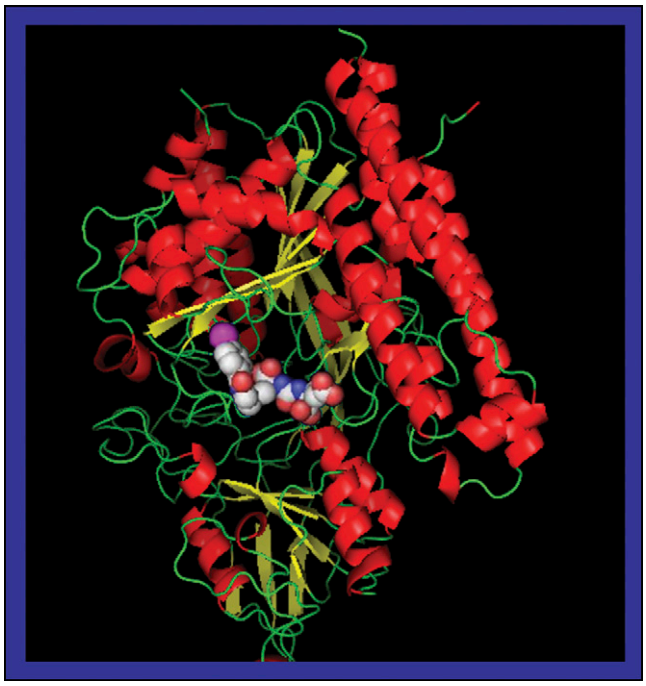

FIGURE 4. Artist's depiction of adhesion of an antigen, drug, or neurotransmitter to a specific site on a molecule, the interaction that provides the basis for molecular medicine and molecular imaging.

Preclinical Studies

At this meeting we saw the many ways in which dedicated instruments and procedures continue to be developed for molecular imaging in animals. Molecular imaging is revolutionizing drug design and development, as well as becoming incorporated more and more in university chemistry departments.

Tatsumi et al. [7] from the Osaka University Graduate School of Medicine (Suita, Japan), the Kobe City College of Technology (Japan), and Hitachi Metals, Ltd.–NEOMAX Company (Tokyo, Japan) reported on "Simultaneous ^{11}C-methionine PET and contrast-enhanced MR rat imaging with an integrated PET/MRI system: initial experience." Figure 5 shows the device, and Figure 6 includes the ^{11}C-methionine PET (left), the contrast-enhanced MR (middle), and the fusion (right) images in the rat abdomen.

Momosaki et al. [1523] from Osaka University (Suita, Japan), Sumitomo Heavy Industries Ltd. (Yokosuka, Japan), and Tohoku University (Sendai, Japan) reported on "^{18}F-FDG imaging of mice brain using a high-resolution semiconductor PET camera (Sumitomo MIP-100)." Figure 7 shows the high quality of images obtained with the system.

Truong et al. [808] from the University of California at Los Angeles (UCLA) reported on "An automated system for quantification/analysis of mouse PET images." In this system, both CT and PET images are obtained in the mouse, and the data are then moved through the system until, at the end, biological parameters (such as region of interest [ROI], standardized uptake values [SUVs], attenuation correction, etc.) are displayed on a screen (Fig. 8). The authors noted that routine use of this easily adaptable system and software is "expected to shorten image analysis time of mouse PET studies by more than an order of magnitude."

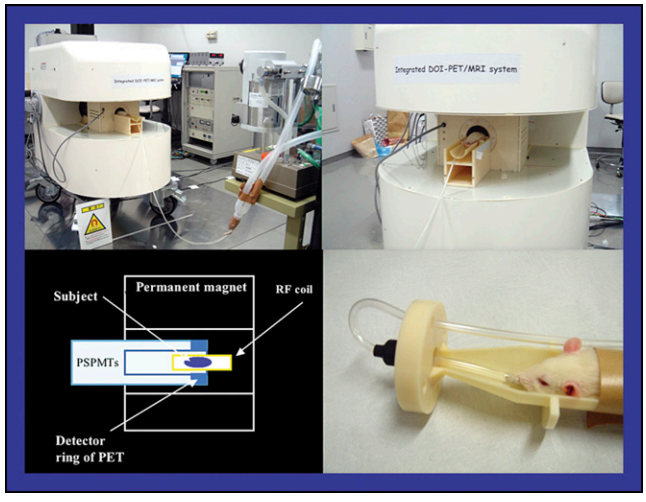

FIGURE 5. Top, 2 images of the integrated PET/MR preclinical device; bottom left, diagram of components; bottom right, rat positioned in gantry.

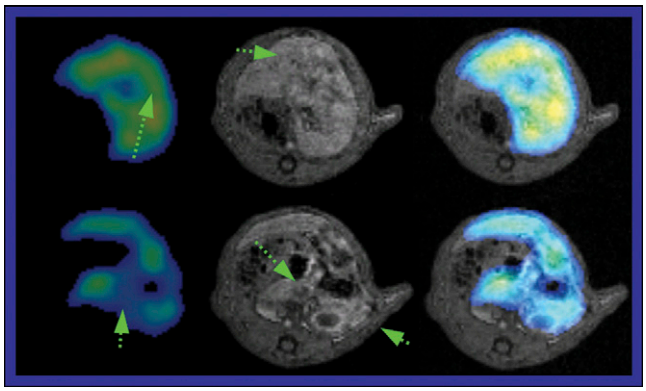

FIGURE 6. Transaxial images of rat abdomen acquired with the device in Figure 5. Left row, ^{11}C-methionine PET images; middle row, contrast-enhanced MR images; right row, fusion images.

Automation of technology is one element that is driving the ability of researchers to report on larger numbers of patients. This was a trend that continued at this meeting. In the early days of nuclear medicine, most papers focused on groups of 5 or 10 patients. Today, multicenter trials and automated processes are yielding much broader reports of experience over much larger patient groups, providing definitive evidence for both effectiveness and efficiency in shorter overall time periods.

An illustration of the relationship between genomics and molecular imaging was shown in the study by Ribeiro and a consortium [126] of French researchers on "A multitracer dopaminergic PET study of young onset Parkinson's disease (YOPD) patients with and without parkin mutations." The investigators reported that YOPD patients with parkin gene mutations have less severe clinical disease than those without the mutations. YOPD patients with disease of long duration had ^{18}F-DOPA uptake and both dopamine transporter and D_2 dopamine receptor binding in the striatum similar to that seen in chronically treated late-onset PD patients with disease of long duration.

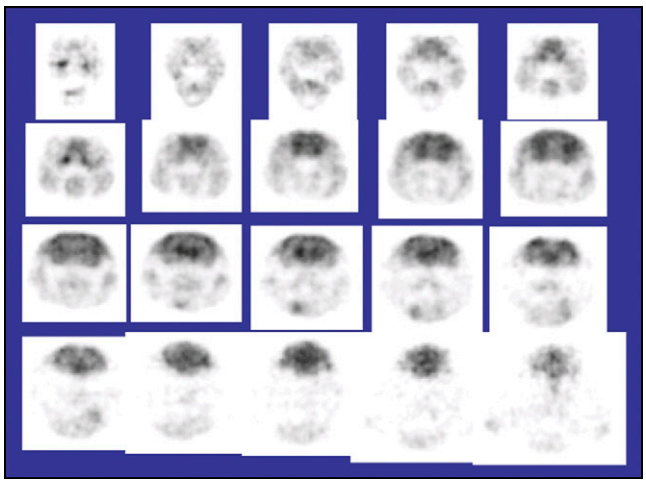

FIGURE 7. Mouse brain images acquired with a high-resolution semiconductor PET camera 45 min after injection of 18.5 MBq of ^{18}F-FDG.

As we all know, pharmaceutical companies charge high prices for new drugs. According to the Congressional Budget Office, these companies now spend 5 times as much as other industries on research and development. Not only is research and development costly, a decade or more of development and trials is required between the initial studies and the entry of a new drug into clinical use. As part of its role in creating a "smarter health care," molecular medicine can contribute to significantly reducing the cost of new drug design and development.

For approval of a new therapeutic drug, the U.S. Food and Drug Administration requires "substantial" evidence of efficacy, demonstrated in controlled clinical trials that assess clinical value. Most studies assess the effect of the new drug on outcome, usually the survival of the patient. It seems clear, however, that approval of drugs and procedures that are used to provide information should be based on their comparative effectiveness in providing new knowledge about the patient and his or her disease. The role of these drugs is analogous to that of instruments that measure body temperature, blood pressure, or blood chemistry. They should be judged by the value of the information they provide.

Guo et al. [263] from the University of Oxford (UK), GlaxoSmithKline (London, UK), and the Imperial College (London, UK) reported on "A bio-mathematical model for radioligand discovery and development." These investigators developed a model to improve efficiency and reduce the attrition rate in radioligand discovery and development. Their model considers entry of the tracer into the brain, specific/nonspecific binding, and the kinetic behavior of the tracer. The authors noted the potential "to predict the in vivo performance of ligands from in silico/in vitro data," a process that would speed the development of imaging probes.

Yang et al. [1610] from the Harvard Medical School and Tufts University (both in Boston, MA) reported on a "Systematic microarray data mining approach useful for identifying cancer imaging targets." This approach (Fig. 9) begins by mining genes overexpressed at a specific tumor and, after a number of steps, results in identification and prioritization of potential radioimaging targets.

At the SNM meeting this year we saw the results of increasing collaboration among industry, professional societies (such as SNM) and academia. For example, a major pharmaceutical company is collaborating with The Ohio State University and a state-funded organization in a $10 million program that combines Ohio State's biomedical imaging research and the company's manufacturing and commercialization expertise.

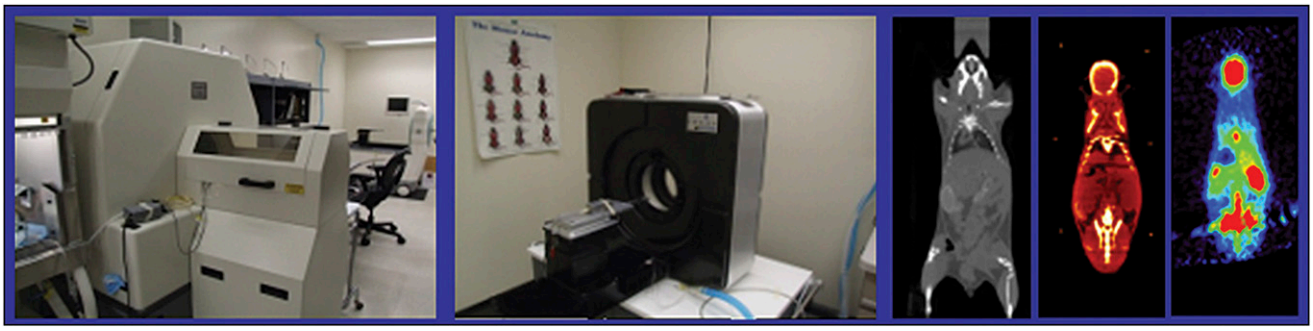

FIGURE 8. An automated system for quantification/analysis of mouse PET/CT images using data from: (A) micro CT and (B) microPET to produce (C) coregistered images (right-hand image). CT and PET image data are warped to the DigiMouse 3D Mouse Atlas (University of Southern California Electrical Engineering).

The New Look of Cancer

Molecular imaging is enabling a new look at cancer. As stated on April 24 in the *New York Times*, the cure for cancer "has a long way to go." The death rate from cancer in the United States has fallen only 5% over the past half century, despite our tremendous strides in scientific understanding.

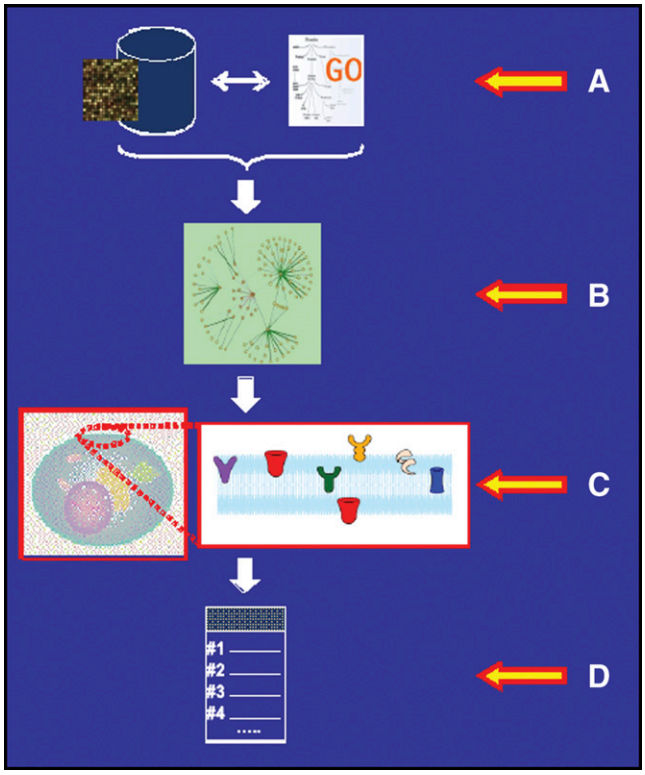

FIGURE 9. The systematic microarray mining strategy for identifying cancer includes the following steps: (A) mining overexpressed genes for a tumor by relevant GO keywords and *Q* value cutoff; (B) enlarging entities by related functions and biomolecular interaction networks; (C) filtering cell surface- and membrane-bound proteins according to subcellular locations; and (D) identifying and prioritizing potential radioimaging targets.

What I call "molecular radiotherapy" was shown at this meeting to be effective in bringing about a complete response—including cure—in many patients, particularly those with lymphomas. I believe that health care reform can be a tipping point that will make this and other successes of molecular medicine more widely known to the public and politicians. Today, if a patient's cancer cannot be removed completely by surgery or successfully treated by external radiation therapy, chemotherapy is the treatment of choice. Chemotherapeutic agents slow tumor progression and can prolong life, but not all cancer cells are killed. Radionuclide therapy can often kill all the tumor cells, because the emitted radiation extends beyond the radiolabeled molecules and hits a larger zone of diseased cells. This is a key advantage of radioactive drugs.

Every year I present what we all now call the "Image of the Year." The image I chose this year comes from a study by Iagaru et al. [47] from Stanford University Medical Center (CA) and shows that molecular radiotherapy can cure non-Hodgkin lymphoma (NHL). The study was titled "^{131}I-tositumomab (Bexxar) vs. ^{90}Y-ibritumomab (Zevalin) therapy of non-Hodgkin lymphoma." The Image of the Year (Fig. 10) shows 2 studies of a 36-y-old woman with NHL. On the left the pretreatment image shows the lesions associated with NHL, and the image on the right shows complete disappearance of those lesions. The study focused on patients who had relapsed after conventional chemotherapy and then underwent either the ^{131}I-tositumomab or ^{90}Y-ibritumomab radioimmunotherapy (RIT) regimen. Eleven of 31 (35.5%) patients treated with ^{131}I-tositumomab had complete responses (without symptoms or other manifestations of disease at follow-ups ranging from 6 mo to several years), and only 4 of 31 (12.9%) showed disease progression. Fifteen of 36 (41.7%) patients treated with ^{90}Y-ibritumomab showed complete responses (many of which were complete cures), and only 4 of 36 (11.1%) showed disease progression. We need to educate physicians, political leaders, and the public about the potential of

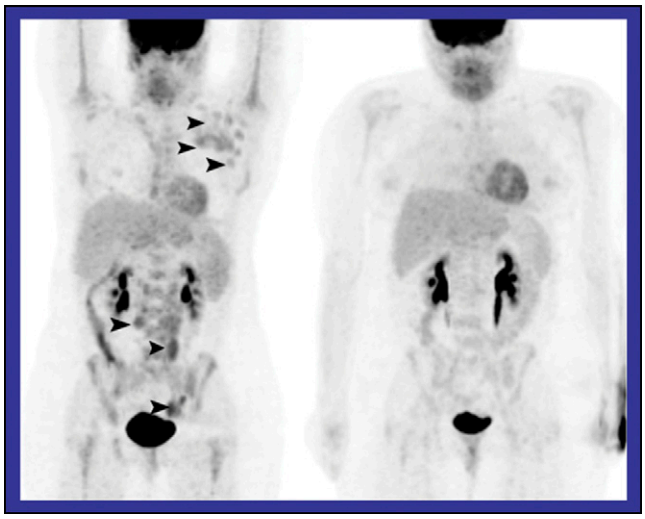

FIGURE 10. 2009 Image of the Year. Images acquired before (left) and after (right) ^{90}Y-ibritumomab therapy in a 36-y-old woman with non-Hodgkin lymphoma, showing complete response.

RIT as a first-line treatment, not solely in patients who relapse after chemotherapy.

In addition to better outcomes, one potential advantage of RIT—sometimes erroneously described as prohibitively expensive—is cost. Most patients with NHL are first treated with chemotherapy, usually R-CHOP (a combination of the monoclonal antibody rituximab and the drugs cyclophosphamide, doxorubicin, vincristine, and prednisone), and ^{131}I-tositumomab or ^{90}Y-ibritumomab RIT is now given only in cases of relapse after many courses (6 or more) of R-CHOP therapy. The cost of R-CHOP treatment is approximately $33,000/cycle (the total cost including nursing is closer to $40,000/cycle). This means that a 6-cycle R-CHOP treatment, which is quite common (sometimes more than 6 cycles are given), costs $240,000. RIT with ^{131}I-tositumomab or ^{90}Y-ibritumomab costs $135,000, half the cost of R-CHOP therapy. I believe that in the future, RIT could achieve the kind of success in terms of widespread use and acceptance that we have seen in nuclear cardiology.

Goldenberg et al. [574] from the Garden State Cancer Center at the Center for Molecular Medicine and Immunology (Belleville, NJ), Immunomedics, Inc. (Morris Plains, NJ), and IBC Pharmaceuticals, Inc. (Morris Plains, NJ) reported that "Combination anti-CD20 immunotherapy and pretargeted anti-CD20 RIT of NHL shows improved efficacy." This comparative effectiveness research study showed that pretargeted RIT improved therapeutic response and reduced hematopoietic toxicity more than immunotherapy alone in mice. Moreover, the addition of consolidation therapy with the anti-CD20 monoclonal antibody veltuzumab significantly improved responses over pretargeted RIT alone.

Several studies were presented on the ability of ^{18}F-FDG PET/CT to monitor treatment in pediatric patients with lymphoma. London et al. [1383] from the Children's Hospital at Westmead (Sydney, Australia) and the University of Sydney (Australia) reported on a retrospective study of "FDG PET/CT in pediatric lymphoma." The utility of PET/CT in children with Hodgkin disease and NHL was compared with that of conventional imaging. PET/CT was found to have a sensitivity and specificity of 95.9% (range, 89.2%−98.7%) and 99.7% (range, 99.4%−99.8%), respectively, compared with conventional imaging, which had sensitivity and specificity of 70.1% (range, 59.8%−78.8%) and 99.0% (range, 98.6%−99.3%), respectively. Figure 11 is an example of a good response after therapy in this study. A lesion with an SUV of 3.9 remained in the proximal left femur. Although this was diminished from the earlier image (which showed an SUV of 11.3), the question was whether it was the result of residual NHL or represented bone repair. Biopsy revealed necrotic bone but no malignancy.

A study of the "Role of ^{18}F-FDG PET/CT in pediatric malignant lymphoma" was reported by Riad et al. [640] from the Children's Cancer Hospital (Cairo, Egypt), the National Cancer Institute (Cairo, Egypt), and St. Vincent's Catholic Medical Centers of New York (NY). Their work

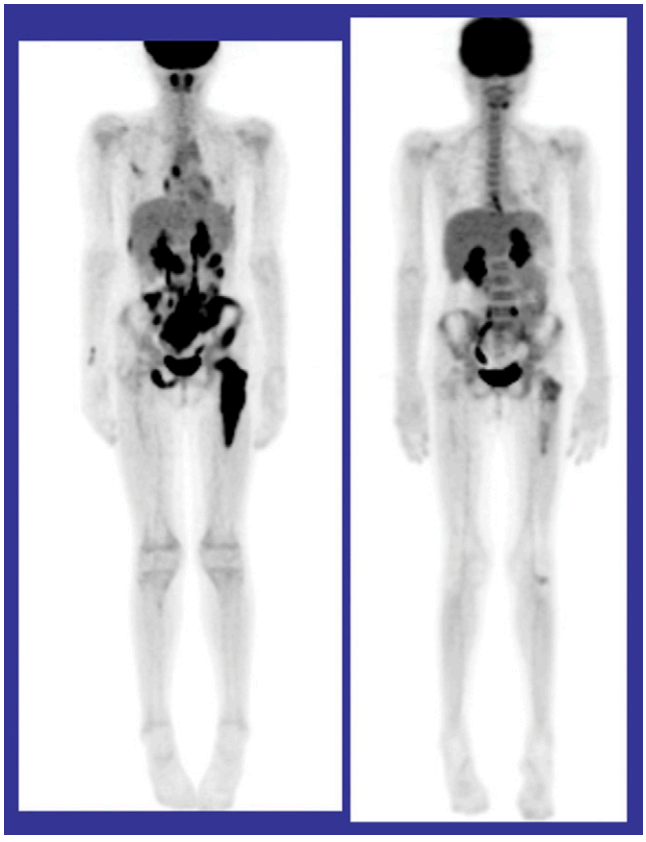

FIGURE 11. ^{18}F-FDG PET images before (left) and after (right) therapy in pediatric lymphoma. The remaining lesion (SUV = 3.9) in the proximal left femur after treatment was determined to represent necrotic bone with no malignancy.

was carried out at the Children's Cancer Hospital in Cairo and described ^{18}F-FDG PET imaging that led to a change in care in 23% of patients in the study. The authors concluded that PET/CT in pediatric malignant lymphoma is more accurate than conventional imaging and recommended that PET/CT should be the first modality for initial staging, evaluating of treatment response, and follow-up in this setting.

Cistaro et al. [1384] from IRMET and the Regina Margherita Infant Hospital (both in Turin, Italy) reported on the "Role of ^{18}F-FDG PET/CT in oncologic pediatric patients: A single centre experience." PET/CT confirmed recurrence of malignancy in 35 of 52 patients with a wide variety of cancers. In 14 patients, malignancy recurrence was excluded. PET/CT modified the therapeutic approach in 14% of the patients. The authors added that PET/CT also identified the more accessible active sites for biopsy and, in the 11 cases of lymphoma in the study, PET/CT improved staging in 7 patients.

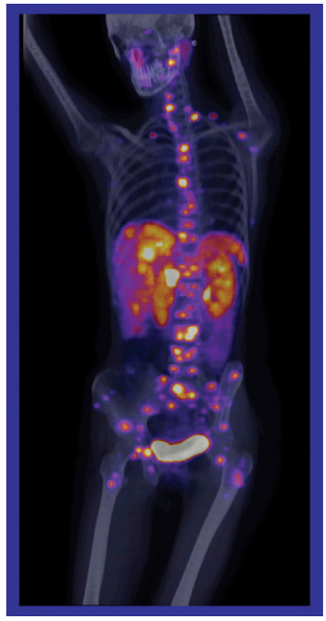

FIGURE 12. Whole-body PET/CT provides an opportunity to study the distribution of neuroendocrine tumors and to monitor a growing range of therapeutic approaches.

Exploring New Tracers

^{68}Ga tracers for PET are becoming popular. ^{68}Ga is available by generator, and house preparation of these tracers is possible without cyclotrons. New generators are being developed, as are freeze-dried kits. The nuclide is well suited for radiolabeling peptides. Current preclinical experience presented at this meeting is defining the clinical indications for ^{68}Ga PET.

Tworowska et al. [376] from the RITA Foundation, RadioMedix, Inc., and the University of Texas M.D. Anderson Cancer Center (all in Houston, TX) reported on the use of "^{68}Ga-glucosamine analogs for PET imaging of cancer." Some of the newer compounds being explored in this area include: DOTATOC, DOTATATE, DOTA-NOC, DOTA-NOC-ATE, DOTA-BOC-ATE, and DOTA-BOM, as well as ^{68}Ga-labeled bombesin, melanocortin peptides, cholecystokinins, neurotensin, and substance P. In in vitro studies, the Texas investigators showed significant accumulation of a ^{68}Ga-labeled glucosamine derivative in human colon cancer (LS174T) and human lung cancer (A549) cell lines. This tracer showed tumor uptake comparable to that of ^{18}F-FDG in tumor-bearing animal models. No significant uptake was observed in heart and brain, a potential advantage over ^{18}F-FDG. The authors concluded that ^{68}Ga-labeled glucosamine derivatives "may be a broad-use, low-cost alternative for PET imaging of tumors."

Beauregard and Hicks [1657] from the Peter MacCallum Cancer Centre (Melbourne, Australia) reported on a "Comparison of neuroendocrine tumor lesions uptake on ^{68}Ga-octreotate PET/CT and post-therapy ^{177}Lu-octreotate SPECT/CT" (Fig.12). In Figure 13, the pretherapy image (left) with ^{68}Ga-octreotate PET/CT shows multiple lesions, and the posttherapy image with ^{177}Lu-octreotate SPECT/CT shows the disappearance of all the lesions. The authors concluded that ^{68}Ga-octreotate PET/CT is effective for planning, dosimetry, and monitoring response of ^{177}Lu-octreotate therapy in patients with somatostatin receptor–positive neuroendocrine tumors.

Fahey et al. [536] from Children's Hospital Boston/Harvard Medical School (MA), the University of Washington (Seattle), and St. Jude's Children's Research Hospital (Memphis, TN) reported on "Variation in ^{68}Ga-PET quantitation within a multicenter consortium." The 10-member Pediatric Brain Tumor Consortium imaged a ^{68}Ge/^{68}Ga-based standard phantom and compared site-based quantitation and central analyses. These yielded

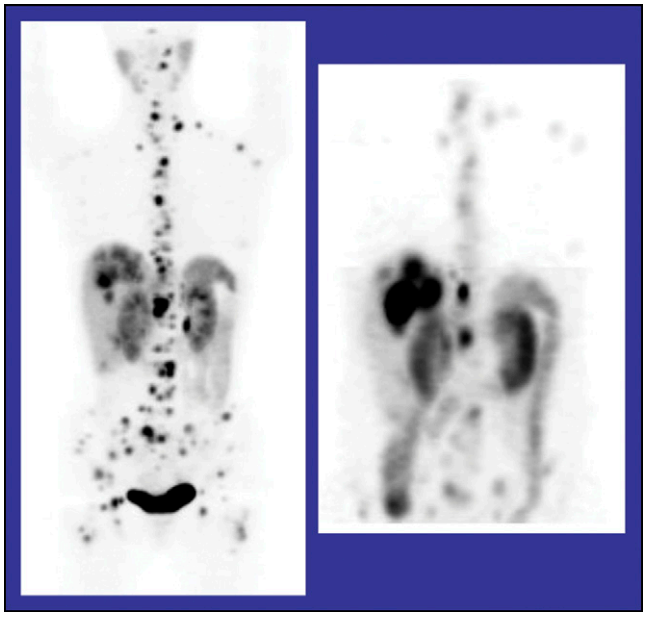

FIGURE 13. Left, pretherapy ^{68}Ga-octreotate PET/CT in a patients with somatostatin receptor–positive neuroendocrine tumors; right, posttherapy ^{177}Lu-octreotate SPECT/CT.

similar results in mean values of recovery coefficients and SUVs. Central analyses provided substantially lower variation in analysis than did the locally analyzed results (range of mean SUV coefficient of variation of 5%−10% and 11%−18%, respectively).

The study by Czigner et al. [1658] from the National Institute of Oncology and Positron Diagnostics, Ltd. (both in Budapest, Hungary) examined "The impact of PET/CT in radiotherapy treatment planning." The researchers performed PET/CT imaging as part of staging in 300 patients and of radiation therapy contouring in 53 patients with a variety of cancers (head and neck cancer, lung cancer, lymphoma, sarcoma, and gynecologic or intestinal recurrences). In more than half of these 53 patients, PET/CT resulted in changes in target volume, target region, and/or dose level.

Another paper on guided therapy was that by Ahmadzadehfar et al. [1662] from University Hospital Bonn (Germany) on "The significance of ^{99m}Tc-MAA SPECT-CT liver perfusion imaging in treatment planning for ^{90}Y microsphere selective internal radiation treatment." In this 73-patient study, the sites of injection of the therapeutic microspheres were changed in many patients because of the finding of extrahepatic infusion. SPECT/CT correctly enabled this finding in 26% of patients in the study, whereas planar imaging identified only 9% and SPECT alone identified only 10% of these patients. The authors concluded that information from SPECT/CT may lead to a change in initial treatment plan, with special significance for sparing normal liver parenchyma and protection of the gallbladder and gastroenteropancreatic system.

Screening, Prediction, and Prognosis

A study by Minamimoto et al. [1372] and a consortium of Japanese researchers from Yokohama City University, the Institute of Biomedical Research and Innovation (Kobe), the Nishidai Clinic Diagnostic Imaging Center (Tokyo), the Atsuchi Memorial Clinic PET Center (Kagoshima), and Tohoku University (Sendai) reported on "Performance profile of FDG PETand PET/CT for cancer screening on the basis of a Japanese nationwide survey between 2005 and 2007." A mind-boggling 126,103 asymptomatic individuals who underwent ^{18}F-FDG PET or PET/CT screening tests were included in the study. Of these, 1,499 (1.19%) were found to have cancer. Of these 1,499, PET or PET/CT studies were abnormal in 78% (0.93% of the total population screened). Cancers of the colon/rectum, thyroid, lung, and breast were found most frequently. These numbers force us to ask about the cost effectiveness of such screening. According to my calculations (which are approximations), assuming that a PET study costs $1,000, then the cost of detecting each unsuspected cancer would be about $100,000.

Many groups are doing whole-body imaging, which makes the topic of incidental findings of growing importance. Zhao et al. [1688] from Fudan University (Shanghai, China) reported on the "Clinical significance of ^{18}F-FDG PET/CT imaging in detecting incidental second primary malignant neoplasms in breast cancer patients." The study included 625 patients with known breast cancer who had undergone ^{18}F-FDG PET/CT imaging. Twenty-four patients (3.84%) were diagnosed as having a second malignant neoplasm (lung, colorectal, stomach, ovarian, thyroid, and pancreatic cancers and lymphoma). Figure 14 shows a patient who, in addition to breast cancer, was found to have an adenocarcinoma in the right lung.

Yoshida et al. [1135] from Asahi General Hospital, Chiba University Graduate School of Medicine, and Tokyo Women's Medical University (all in Chiba, Japan) reported on "Assessment of new risk factors for atherosclerosis at FDG PET/CT in healthy subjects." Figure 15 shows lesions found in the ascending and descending aorta in this study. ^{18}F-FDG uptake in the aortic wall (as assessed by total SUV_{max}) was correlated with known cardiovascular risk factors. The authors found that uptake in the aortic wall was significantly associated not only with classic cardiovascular risk factors (body mass index, visceral fat area, triglycerides, blood pressure) but also with new factors (such as ferritin and adiponectine levels).

Rominger et al. [9] from the University of Munich (Germany) reported that "^{18}F-FDG PET-CT identifies patients at risk for future cardiovascular events in an otherwise asymptomatic cohort suffering from neoplastic disease." The authors sought to determine the correlation of arterial wall tracer uptake and calcification as assessed by PET/CT with subsequent occurrence of cardio- and cerebrovascular events in cancer patients without symptoms of vascular disease. Out of 1,000 patients who underwent PET/CT, 15 experienced a cardio- or cerebrovascular event over a mean follow-up of 29 mo. After analysis of imaging results in these patients and a group of patients who did not experience such events, the researchers identified a strong association between increased arterial wall ^{18}F-FDG uptake and increased atherosclerotic plaque burden. They concluded that PET/CT "could identify high-risk patients in need of further cardiovascular diagnostics or intensified medical therapy."

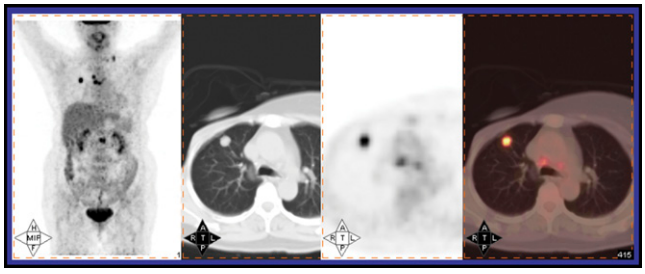

FIGURE 14. ^{18}F-FDG PET/CT imaging (left) as part of treatment management in a patient with breast cancer identified an incidental adenocarcinoma in the right lung (right 3 images).

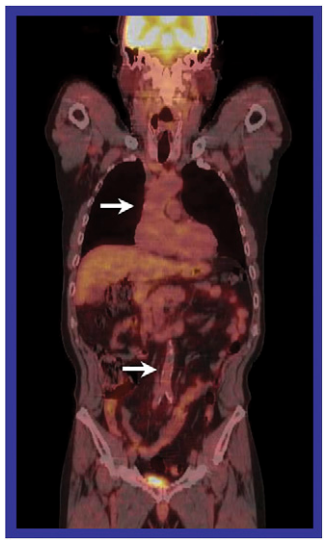

FIGURE 15. Example of incidental findings in PET/CT screening studies in presumed-to-be-healthy participants. Lesions were identified in the ascending and descending aorta (arrows).

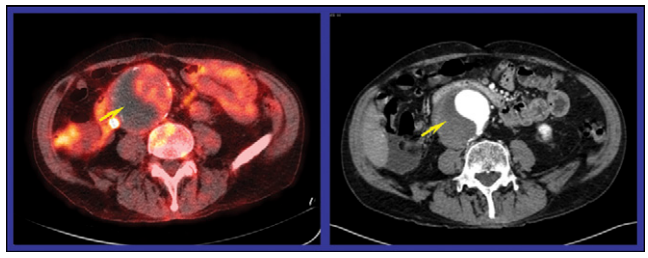

FIGURE 17. In this patient from the same study as Figure 16, uptake of ^{18}F-FDG in a 7.2-cm ascending aortic aneurysm with a cold region within the vessel on PET (left) suggested the presence of thrombus, as confirmed on contrast CT (right).

Muzaffar et al. [1325] from St. Louis University (MO) reported on "Incidental diagnosis of thrombus within an aneurysm in FDG PET/CT: Frequency in 926 patients." Retrospective review of PET/CT imaging for known or suspected cancers revealed an incidental, unsuspected aortic aneurysm in 21 (2.3%) of these patients. Of these 21, 10 had ^{18}F-FDG PET/CT findings suggestive of the presence of a thrombus. Seven of these 10 (70%) were confirmed by contrast CT (3 had no follow-up). Figure 16 shows an example of diffuse uptake of ^{18}F-FDG in an aortic aneurysm, with no evidence of thrombus (i.e., no cold region within the lesion). Figure 17 shows the PET/CT image in an aneurysm with a cold region within the vessel, highly suggestive of thrombus (and confirmed on CT).

Itskovich et al. [1682] from the University of Arkansas Medical School (Little Rock), the Myeloma Institute for Research and Therapy (Little Rock, AR), and Cancer Research and Biostatistics (Seattle, WA) reported on the "Utility of FDG PET/CT in detecting extramedullary disease in multiple myeloma patients." ^{18}F-FDG PET/CT detected extramedullary disease at 33 sites in 19 (6%) of 303 patients imaged. This use in multiple myeloma has been approved. Figure 18 is an image of disease detected in the paratracheal node.

The number of lesions on PET/CT is associated with prognosis in patients with multiple myeloma. Bartel et al. [644] from the the University of Arkansas Medical School (Little Rock), the Myeloma Institute for Research and Therapy (Little Rock, AR), and Cancer Research and Biostatistics (Seattle, WA), reported on "Focal lesion number and SUV on FDG-PET/CT as they related to event-free survival and overall survival in multiple myeloma patients." The authors found that untreated patients with <6 focal lesions on PET/CT had better outcomes. Overall, SUV^{max} was an independent prognostic factor. PET/CT was useful for detecting extramedullary disease, which predicted a higher risk of relapse. They concluded that these findings support routine incorporation of ^{18}F-FDG PET/CT into the diagnostic work-up for staging of multiple myeloma patents as well as in prognostic and therapeutic response assessment. Figure 19 shows patients with increasing numbers of focal lesions.

Giacomuzzi et al. [336] from the Azienda Ospedaliero Universitaria (Udine, Italy) reported on "Clinical significance of FDG PET-CT unexpected thyroid focal findings: Our experience in 5,000 patients studied for known or

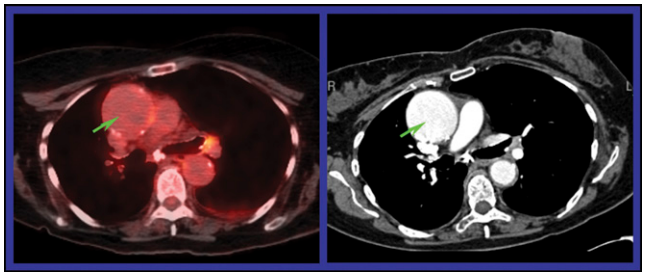

FIGURE 16. Retrospective review of PET/CT studies revealed incidental aortic aneurysms in 2.3% of patients. In this patient with a 5.8-cm ascending aortic aneurysm, absence of thrombus as indicated by a lack of a cold region within the lesion on PET (left) was confirmed on contrast CT (right).

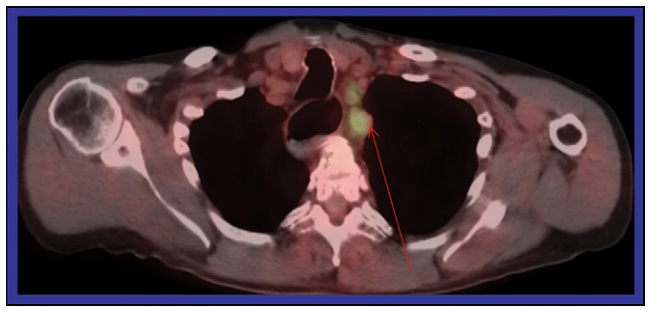

FIGURE 18. ^{18}F-FDG PET/CT detected extramedullary disease in the paratracheal node in this patient with multiple myeloma.

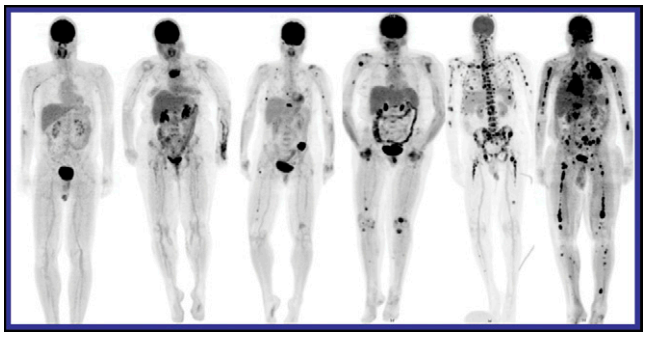

FIGURE 19. The severity of lesions at baseline ^{18}F-FDG PET in multiple myeloma was correlated with outcome. From left to right, these patients were found to have no, >5, >10, >20, >50 and >70 focal lesions, respectively.

suspected nonthyroid cancer." Of the 5,000 patients imaged for nonthyroid malignancies, 94 (1.5%) had focal uptake of tracer in the thyroid. Seventy-one of these patients underwent follow-up examinations. Cancer was confirmed in 19 of these patients (27%), with benign conditions in the remaining 52 (73%).

Iagaru et al. [133] from Stanford University (CA) presented an interesting paper describing "A novel strategy for a cocktail ^{18}F-fluoride and ^{18}F-FDG PET/CT scan for evaluation of malignancy: Results of the pilot phase study." ^{18}F-FDG can fail to accumulate in some lesions as a result of variable rates of glucose metabolism, a problem that this dual-tracer approach attempts to resolve. Figure 20 shows ^{18}F-FDG, sodium ^{18}F-fluoride, and combined images in a 75-y-old man with prostate cancer. The combined administration of the 2 tracers, followed by a single PET/CT study, is feasible and could result in improved patient care and reduced costs. I think that it is probable, particularly in the face of current supply problems with tracers such as ^{99m}Tc, that fluoride imaging of the skeleton is likely to increase and that we are likely to see more beneficial imaging "cocktails" that incorporate its benefits.

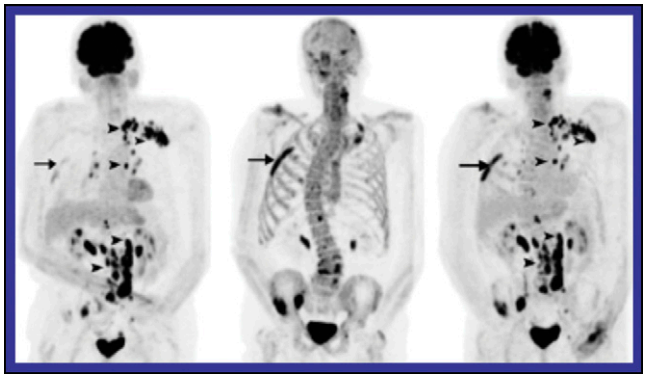

FIGURE 20. ^{18}F-FDG (left), ^{18}F-fluoride (middle), and combined images (right) in a 75-y-old man with prostate cancer.

Reducing Cost in Health Care Reform

Perkins et al. [335] from the Indiana University School of Medicine (Indianapolis) defined the "Optimal PET/CT anatomic coverage for staging and diagnosis of head and neck cancer." The retrospective study looked at 627 PET/CT torso scans acquired in patients with head and neck cancer. The authors found that anatomical coverage for initial staging and diagnosis needs to extend only down to the level of the aortic arch (analogous to the areas imaged in standard CT and MR imaging). An extended torso scan provided little additional clinical value, affecting only 1.8% of the studies. This "limited coverage" protocol reduces scan time, radiation dose, and cost without negatively affecting patient care.

Costs are being decreased by the use of specialized imaging devices. Spanu et al. [1696] from the University of Sassari (Italy) reported on the "Role of ^{99m}Tc-tetrofosmin molecular breast imaging in patients with breast lesions." In 321 consecutive patients with breast lesions, molecular breast imaging had a sensitivity of 95.6% (90.4% in patients with lesions ≤10 mm; 99% in patients with lesions >10 mm). Molecular breast imaging was more specific than mammography, which had a specificity of 86.4%. Most benign lesions were negative on molecular breast imaging, even when mammography had indicated suspicious findings. Figure 21 shows images acquired by the University of Sassari researchers using the dedicated

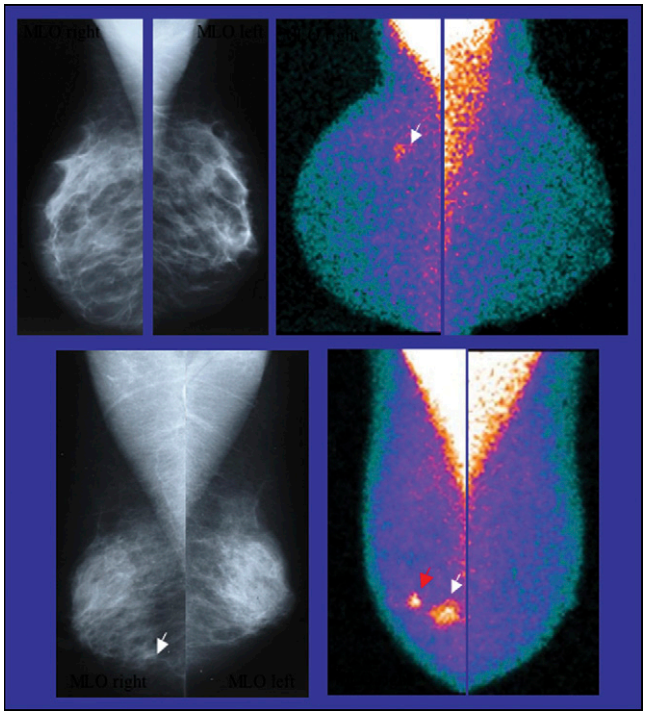

FIGURE 21. Left, conventional mammography; and right, molecular breast images acquired using the LumaGEM dedicated breast camera, with spatial resolution of 1.6 mm and energy resolution of 4.6% at 140 Kev.

LumaGEM 3200S/12K (Gamma Medica-Ideas, Inc., Northridge, CA).

Baghaei et al. [350] from the University of Texas M.D. Anderson Cancer Center (Houston) reported on "A breast lesion study with a high-resolution transformable PET camera." The HOTPET has a resolution better than 3 mm and can be transformed between breast mode and whole-body mode. The HOTPET camera consists of 12 independent modules (Fig. 22). Figure 23 shows sample images of a 4.95-mm lesion in a phantom. When imaging was carried out in the whole-body mode, the SUV was 5.5; in the breast mode, the SUV was 2.5.

Cardiology

At this meeting 26 of 187 presentations in cardiology involved ^{82}Rb. Ziadi et al. [73] from the University of Ottawa Heart Institute (Canada) reported on "Characterization of patients with preserved and reduced myocardial flow reserve measured using ^{82}Rb PET." The study included 468 patients who underwent pharmacologic stress PET imaging. Data acquisition was in listmode, which made possible dynamic and gated imaging. The researchers found that patients with normal perfusion scans but abnormal (reduced) myocardial flow reserve also had conditions known to alter vascular reactivity (e.g., greater age, diabetes, elevated systolic blood pressure). Early detection of microvascular disease as indicated by reduced myocardial flow reserve could enable earlier and more effective therapy.

Javadi et al. [27] from the Johns Hopkins University (Baltimore, MD) reported on the "Relationship between plaque burden, coronary flow reserve, and cardiac events in hybrid ^{82}Rb PET-CT." The study included 75 patients who underwent rest/dypiridamole perfusion ^{82}Rb PET/CT imaging followed by CT angiography. The authors found that 38% of patients with subclinical atherosclerosis had coronary flow reserves equal to or less than those in patients with clinically overt disease ischemia. The authors concluded that because low coronary flow reserve may occur in the absence of visually abnormal PET perfusion and with relatively low CT angiographic plaque that "flow quantification may provide incremental information for risk stratification in hybrid cardiac PET/CT."

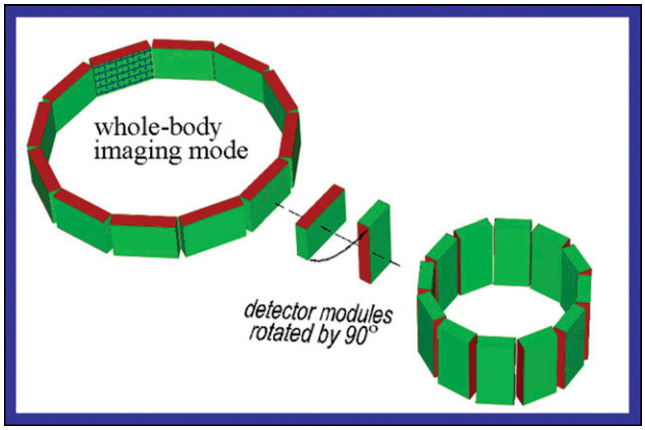

FIGURE 22. The HOTPET high-resolution transformable camera is made up of 12 independent modules.

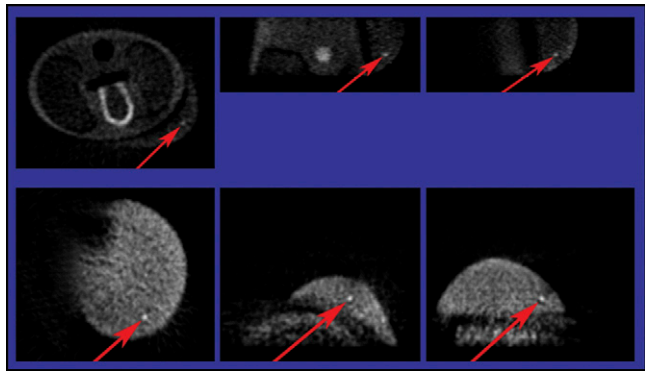

FIGURE 23. Transverse (left), coronal (middle), and sagittal (right) images of a 4.95-mm breast lesion in a phantom, acquired with the HOTPET camera. Top row was acquired in whole-body mode, in which the lesion standardized uptake value was 5.5. Bottom row was acquired in breast mode, in which the lesion standardized uptake value was 2.5.

One question this and other studies raise is whether everyone over a certain age should undergo assessment of coronary plaque burden and coronary flow reserve to identify possible future problems. This reminds me in some ways of the situation with stress electrocardiography, which was and probably still is used as a screening test. We are seeing more radiotracer-based studies that can predict disease and identify those individuals who may develop specific diseases in the future.

Less Invasive Tests

The number and types of minimally invasive tests are increasing. Herzog et al. [25] from the University Hospital Zurich (Switzerland) reported on "Low-dose and fast hybrid cardiac imaging: New method combining CT angiography (CTA) and SPECT." In 40 patients, SPECT/CTA predicted the need for coronary revascularization with a sensitivity, specificity, and positive and negative predictive values of 100%, 96.0%, 100%, and 93.8%, respectively, when evaluated against the results of subsequent invasive coronary angiography. The radiation doses were significantly lower with SPECT/CTA than with invasive coronary angiography. Figure 24 shows the beautiful images obtained with this approach. This is another example of comparative effectiveness research. Invasive coronary angiography could have been avoided in 60% of the patients, resulting in great cost savings.

A number of new PET tracers are being developed to study the heart, including tracers for myocardial perfusion. Maddahi et al. [184] from UCLA, Johns Hopkins (Baltimore, MD), Lantheus Medical Imaging (Billerica, MA), and Cardiovascular Imaging Technologies (Kansas City, MO) reported on a "Phase 1 rest-stress study of ^{18}F-

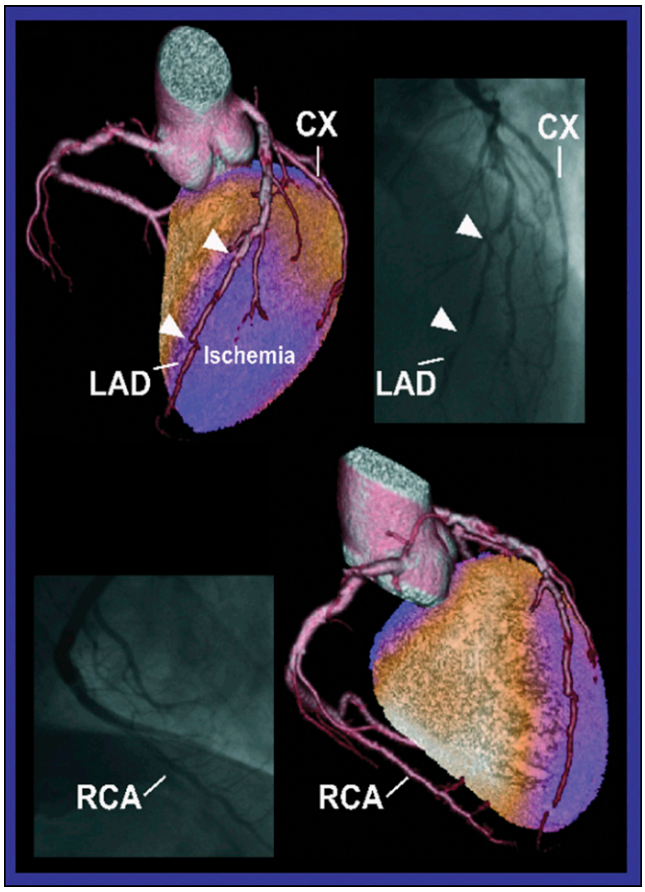

FIGURE 24. Images obtained with SPECT/CT angiography (top left and bottom right) accurately predicted the results of subsequent invasive angiography (top right and bottom left).

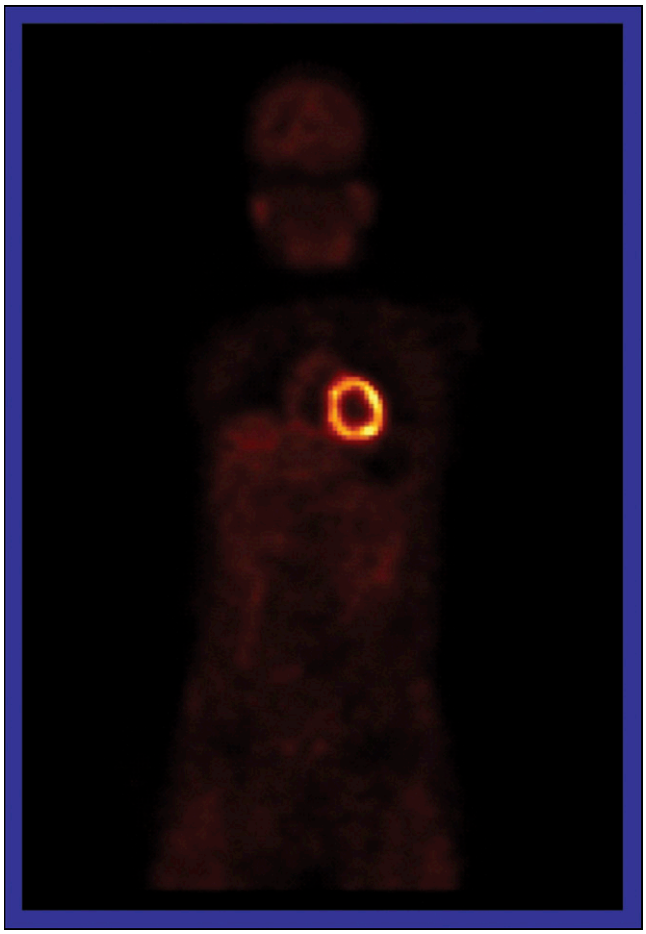

FIGURE 25. Whole-body image acquired with the myocardial perfusion PET tracer ^{18}F-BMS747158.

labeled BMS747158 myocardial perfusion PET tracer: Human safety, dosimetry, biodistribution, and myocardial imaging characteristics." Figure 25 shows a whole-body image acquired using ^{18}F-BMS747158. Stress imaging is feasible with both treadmill exercise and pharmacologic stimulation with adenosine. The myocardium can be clearly visualized for several hours after rest and stress injection. A 5-min gated acquisition started 2 min after injection yields high-quality images. This is an example of a large amount of information obtained in a very short period of time.

Groves et al. [599] from University College London (UK) and Nottingham University Hospital (UK) reported on "First experience of combined cardiac PET/64-detector CTA with invasive angiographic validation." PET/CTA showed enhanced diagnostic performance over CTA alone, even when CTA was interpreted by an expert. Figure 26 shows cardiac PET/64-detector CTA and CTA alone.

Some advantages accompany the performance of myocardial perfusion imaging in patients who are in a sitting position. Lang et al. [70] from the Center for Nuclear Medicine Ltd. and the Charles University (both in Prague, Czech Republic) reported on "Myocardial perfusion images acquired in sitting patients: comparison with supine position." Figure 27 shows both the supine and sitting Nucline (Mediso Medical Imaging Systems; Budapest, Hungary) devices used by this group. The advantages of the sitting approach can be seen in patients in heart failure who cannot lie down for long periods of time or cannot lie down at all and also for obese patients who do not fit into a conventional device. Image patterns of myocardial perfusion are different depending on whether the data are acquired in the supine or the sitting position. Parameters of quantitative analysis differ significantly, so that current commercially available normal databases should not be used for quantitative analysis of images acquired in sitting patients.

Maddahi et al. [598] from UCLA and Digirad Corporation (San Diego, CA) reported on "Clinical evaluation of low-dose X-ray–based transmission imaging for attenuation correction of SPECT myocardial perfusion images." The upright solid-state system (Fig. 28) produces high-quality transmission scans with greatly reduced patient doses (~5 μSv) and a very low incidence of misregistration. The authors reported on attenuation correction in 108 patients

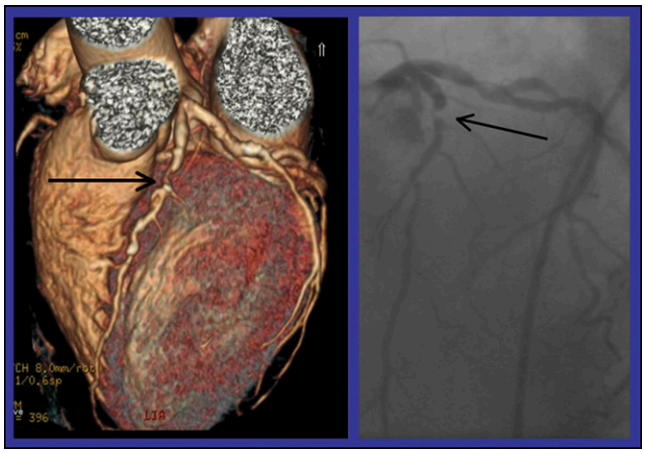

FIGURE 26. The addition of PET improved the diagnostic performance of CT angiography over CT angiography alone. Left, a left anterior descending lesion on CT angiography with PET; right, the same lesion on conventional invasive angiography.

with a low pre-SPECT likelihood of coronary artery disease who underwent same-day rest–stress SPECT with a ^{99m}Tc-labeled agent. In image analysis, regional differences of count rates in the inferior, septal, lateral, and anterior walls of the heart were less after attenuation correction. Breast and diaphragmatic attenuation artifacts were corrected. Radiation dose to the patient from attenuation correction was significantly less than with conventional SPECT/CT.

The Chemistry of Mental Activity

Hans Berger was a pioneer in neurology who used the electroencephalogram at the turn of the 20th century to search for "physical counterparts of mental events." He said that, "Electrical brain activity can be shown to have a significant relationship to mental activity." The "brain/mind" relationship has been a subject of controversy since the discovery of electroencephalography, but it can be clarified by using molecular imaging and its relation to mental activity.

Yoshizawa et al. [1274] from Tokyo Women's Medical University (Japan) reported on "Analysis of brain FDG-PET scans of normal subjects." The study included 128 normal participants (again, a relatively large number of patients as seen in increasing numbers of papers at this meeting). The authors found a significant correlation between aging and brain hypometabolism (Fig. 29). Hypometabolism in the frontal region, including the medial and superior frontal lobes, anterior cingulate gyrus, and superior temporal gyrus, decreased with age. A significant correlation was also found between years of education and brain hypometabolism (Fig. 30) in the superior frontal gyrus and temporoparietal region, especially in the right hemisphere.

Iida et al. [470] from the National Cardiovascular Center (Osaka, Japan), Saitama Medical School (Japan), and Toranomon Hospital (Tokyo, Japan) described a "Three-dimensional realistic brain phantom containing detailed grey matter and bone structures for nuclear medicine imaging." The authors reported on studies

FIGURE 27. Top, Nucline Spirit DHV for supine myocardial perfusion image acquisition; bottom, Nucline CardioDESK for imaging patients in sitting positions.

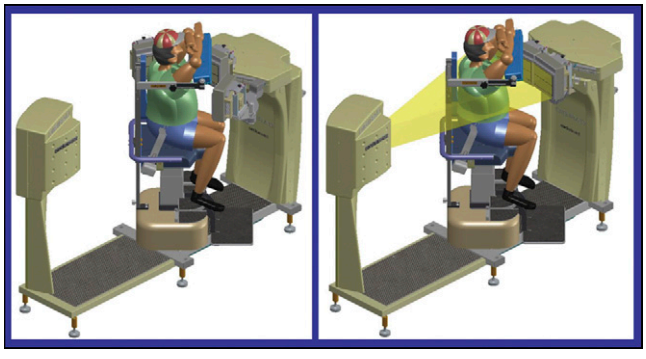

FIGURE 28. Digirad solid-state SPECT for upright myocardial perfusion imaging obtains images in (left) emission mode and (right) transmission mode for attenuation correction.

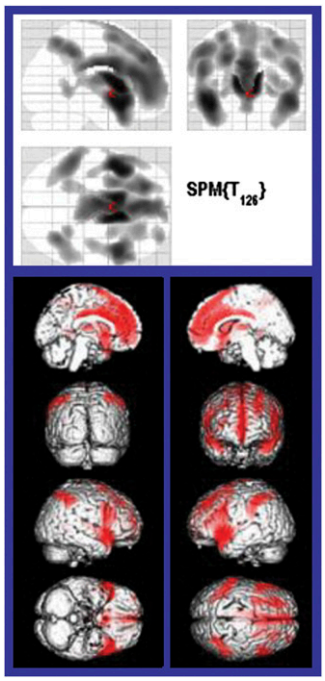

FIGURE 29. Brain ^{18}F-FDG scans in normal subjects found significant correlation between aging and brain hypometabolism. Statistical parametric maps (top) and PET images (bottom) showed that activity in the medial and superior frontal lobe, anterior cingulated gyrus, and superior temporal gyrus decreased with age.

validating initial imaging with this phantom (Fig. 31) and discussed its potential use for evaluating various reconstruction programs.

Nishikawa et al. [1214] from Nihon Medi-Physics Co., Ltd. (Tokyo, Japan), Sapporo Azabu Neurosurgical Hospital (Japan), Hyogo Brain and Heart Center (Himeji, Japan), and the University of Washington (Seattle) reported on "An automated ROI setting method using NEUROSTAT and the VOI template for brain function areas." Figure 32 shows the results of automation of analysis on data from a 70-y-old woman with mild clinical impairment. The authors found that this automated ROI setting method can be "effectively applicable for early diagnoses and severity assessments of Alzheimer disease with minimal loss of anatomical information." Direct comparison/evaluation of the ROIs is possible with the Z-score mapping and MR images of the same regions over time.

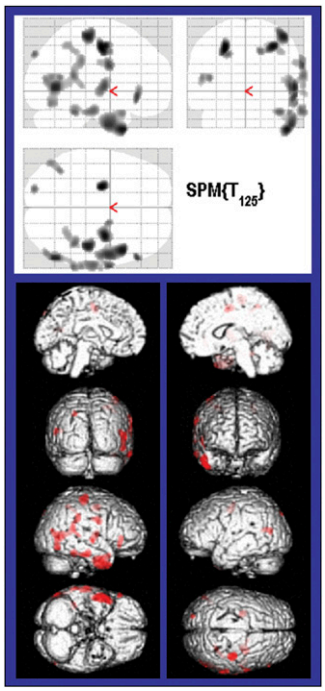

FIGURE 30. Images from the same study as Figure 29 showed significant correlation between years of education and brain hypometabolism. Activity in the temperoparietal region, especially in the right hemisphere, was higher with more years of education.

Odano et al. [807] from Niigata University (Japan), the National Institute of Radiological Sciences (Chiba, Japan), Fujifilm RI Pharma Ltd. (Tokyo, Japan), and the Karolinska Institute (Stockholm, Sweden) reported on "Automated receptor imaging system (ARIS) in neuroreceptor binding studies with PET." Figure 33 shows dopamine transporter images with binding potential and other parameters calculated automatically in about 4 min.

Molecular Neuropharmacology

Joanna Fowler, PhD, known to all of us here for her groundbreaking work on neurotransmitters, neuropharmacology, and radiolabeled imaging at the Brookhaven National Laboratory, said, "You don't know how much of the drug really gets into the human brain. You don't know how fast it gets in. You don't know if inhibition of an enzyme or a receptor persists for a long time or if it's rapidly reversible. You don't have any of that information. You're just guessing. With molecular imaging, you can look directly at what the drug is doing in the human brain. That is an extremely powerful tool."

One-third of all prescription drugs in the United States are administered to affect mental activity, a clear indication that improved drugs with enhanced targeting efficiency in the brain would be both useful and successful. Wang et al. [1284], including Dr. Fowler, from Brookhaven National Laboratory (Upton, NY), UCLA, the National Institute on Alcohol Abuse and Alcoholism (NIAAA)/National Institute on Drug Abuse (NIDA) (Rockville, MD), and the Veterans Affairs Medical Center (Portland, OR), reported that "Dopamine function during early withdrawal predicts recovery in methamphetamine users." They found that dopaminergic function during early withdrawal in methamphetamine users predicted recovery of that dopaminergic function after protracted abstinence. Poor dopaminergic response after oral methylphenidate during early withdrawal in methamphetamine users who relapsed indicated a more severe addictive state. Early detection of the extent of dopaminergic dysfunction may be helpful in predicting the outcome of rehabilitation efforts.

Wang et al. [1282] from Brookhaven and NIAAA/NIDA also reported on "Decreased brain responses during cognitive inhibition of food craving elicited by food stimulation in obese subjects." Hungry obese and nonobese participants were exposed to food stimulation with and without spoken inhibitions against eating. ^{18}F-FDG PET images were acquired. Obese participants were found to have

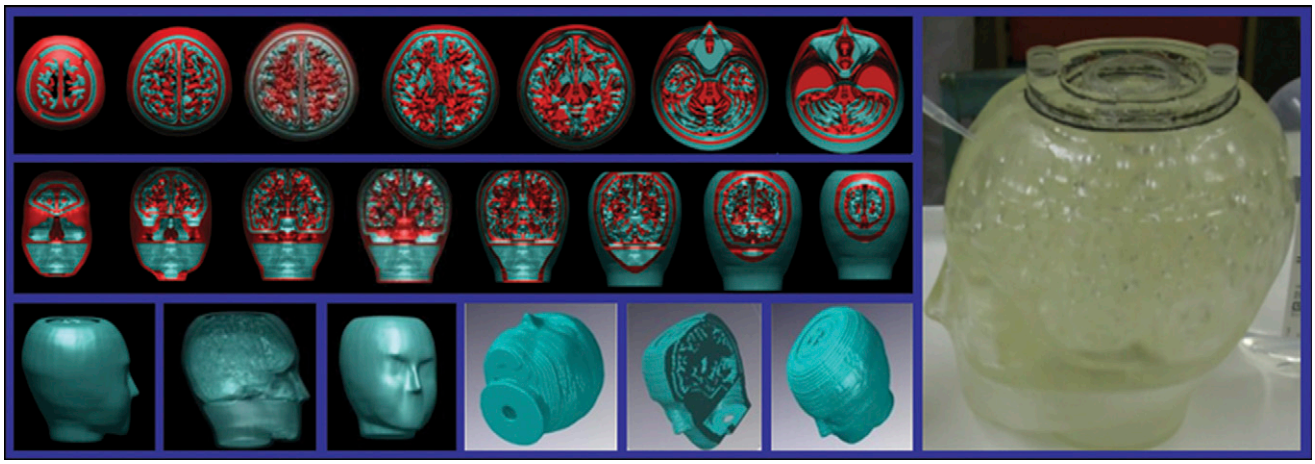

FIGURE 31. A 3-dimensional brain phantom (right) constructed using a laser modeling technique provided consistent results with SPECT, CT, and MR imaging and showed promise for evaluating various reconstruction programs.

lower activation in brain regions involved with motivation and reward during food stimulation than did nonobese participants. During food stimulation, obese patients were also unable to suppress brain activation in regions involved with emotional regulation, conditioning, and motivation (Figs. 34 and 35). The authors concluded that "These results suggest that this is the mechanism by which cognitive inhibition decreases the desire for food, which is consistent with the greater vulnerability of obese individuals to uncontrolled eating when food is readily available." Obesity is another target for those seeking health reform, and the exploration of the underlying brain chemistry mechanisms will surely play a part in finding new solutions.

Substance abuse is a huge area in which molecular imaging and molecular medicine can be applied successfully. Leroy et al. [77] from INSERM-CEA at the Hospital Frédéric Joliot (Orsay, France), the Paul Brousse Hospital (Villejeuf, France), and the Centre Hospitalier d'Orsay (France) reported on "Assessment of dopamine transporter (DAT) availability in tobacco and cannabis addictions with high-resolution PET." The researchers identified a 15%−30% decrease in striatal and extrastriatal dopamine transporter availability in tobacco- and cannabis-dependent participants compared with nonaddicted controls. Cocaine dependence was associated with lower levels of endogenous dopamine (Fig. 36).

We saw examples of dedicated instruments for neuroimaging at this year's meeting. One notable example came from Yamamoto et al. [1532] from Kobe City College of Technology (Japan), the National Center of Neurology and Psychiatry (Tokyo, Japan), and the Institute of Biological Research and Innovation (Kobe, Japan), who reported on "Development of the PET Hat: Wearable PET system for brain research." The device and images are shown in Figure 37. One potential use, in my opinion, for this (or an even simpler device) would be for screening for increased

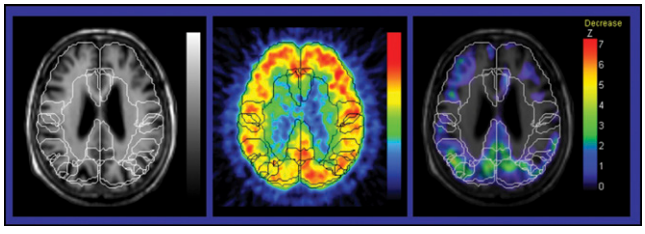

FIGURE 32. Left, MR; middle, ^{18}F-FDG PET; and right, Z-score automated analysis images in a 70-y-old woman with a Mini Mental Status Examination score of 27/30.

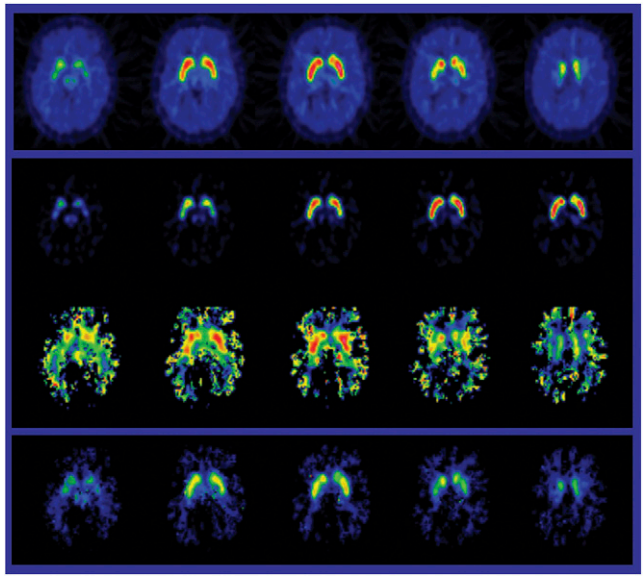

FIGURE 33. Biological parameters were calculated within 4 minutes from ^{11}C-PE21 PET dopamine transporter imaging (top) data. Shown here are binding potential (second row), R_1 (third row), and k_2 (fourth row).

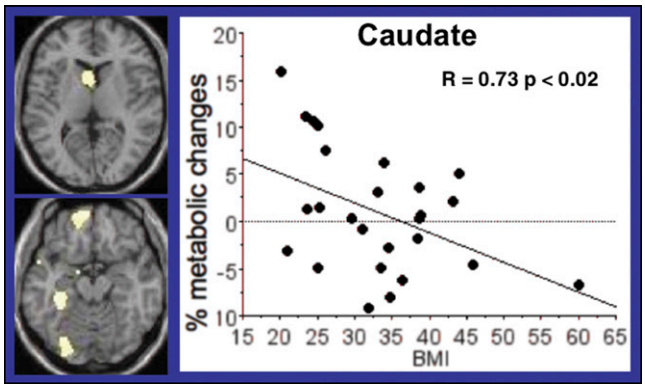

FIGURE 34. Decreased responses were noted in the caudate and orbitofrontal cortex on ^{18}F-FDG PET (left) in obese subjects during food stimulation, with decreasing response tied to increasing body mass index (right).

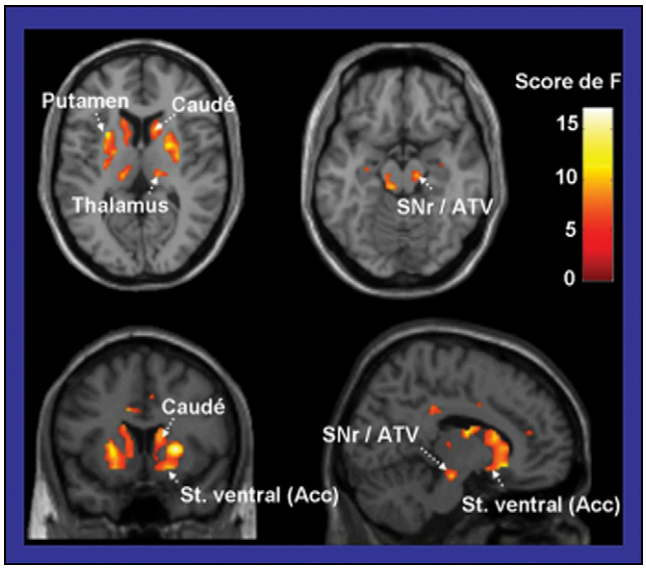

FIGURE 36. High-resolution PET identified a 15%–30% decrease in striatal and extrastriatal dopamine transporter availability in individuals who were tobacco and/or cannabis dependent.

amounts of amyloid plaque in the brains of elderly persons. High spatial resolution is not needed. Specialized simple radiation detection instruments can reduce costs and increase productivity. The spatial resolution of the diagnostic imaging device should match the resolution requirements of the patient's problem. In 1986, I was a member of a group that began to use the 2-detector system shown in Figure 38 to study the duration of occupancy of opiate receptors by naltrexone (Lee et al., *J Nucl Med.* 1988;29:1207–1211). The machine cost about $30,000 to build. We could show that naltrexone blocked the opiate receptors with a mean duration of 12 h, and these studies could be carried out with 20 observations made with the same radiation dose as a single PET scan (in this case the tracer was ^{11}C-carfentanil).

At this meeting, 48 presentations focused on dementia. The Alzheimer's Disease Neuroimaging Initiative of the NIH promotes MR and PET imaging as well as biomarkers in blood and urine to diagnose senile dementia of the Alzheimer type at an early stage and monitor disease progression.

Choi et al. [1190] from the University of Pennsylvania (Philadelphia) and Avid Radiopharmaceutical, Inc. (Philadelphia, PA) reported on "^{18}F-AV-45 (^{18}F-florpiramine): A PET imaging agent for mapping β-amyloid plaques in the brain." ^{18}F-β-amyloid-plaque imaging agents are in phase 3 clinical trials, and we hope that approval comes soon. These agents are especially promising for differentiation among dementias.

Choo et al. [1257] from the Seoul National University College of Medicine (Korea) reported on "Imaging of amyloid plaques and cerebral glucose metabolism in amnestic mild cognitive impairment." The authors explored topographic changes in cerebral glucose metabolism using ^{11}C-PIB PET imaging in normal and amnestic mildly cognitive impaired elderly participants. Figure 39 shows the extent and severity of abnormal ^{11}C-PIB retention. Amyloid deposition in specific cortical areas was correlated

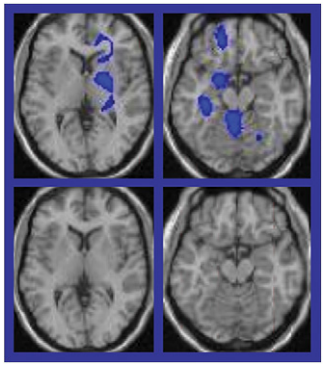

FIGURE 35. Cognitive inhibition of hunger (by talking) led to greater suppression of brain activation in sites associated with hunger in nonobese participants (top row) than in obese participants (bottom row).

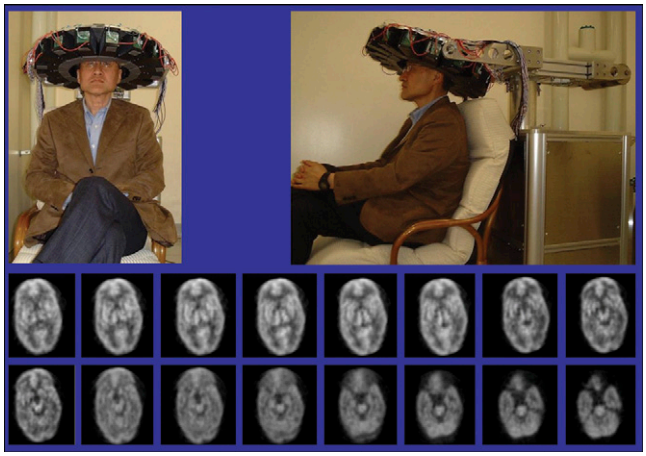

FIGURE 37. Top, PET Hat wearable PET system developed in Japan; bottom, images acquired with the device.

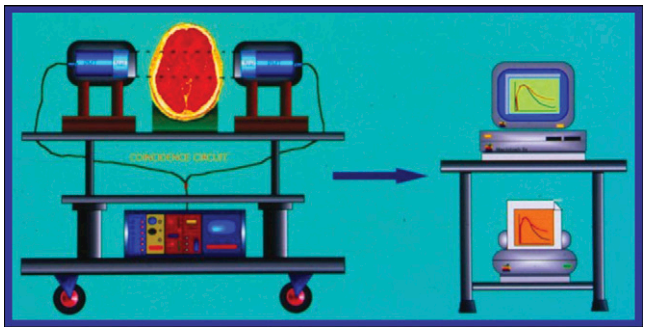

FIGURE 38. Schematic of a dual-detector probe system developed in the 1980s for efficient opiate receptor imaging at low cost.

with hypometabolism in the bilateral precuneus, parietal, and temporal areas.

Frey et al. [251] from the University of Michigan (Ann Arbor) reported on "PET neurochemical vs. clinical phenotypes in mild-early dementia." The researchers evaluated PET neurochemical measures of β-amyloid and nigrostriatal projection integrity in a range of early dementia states. Figure 40 shows comparative results in Alzheimer disease, dementia with Lewy bodies, and frontotemporal dementia. One key finding was that in more than a fourth of patient studies, the PET classification did not agree with the clinical assessment. This is another area in which molecular imaging is providing objective data in a field that has conventionally relied on subjective or physical examinations.

Protas et al. [1414] from UCLA reported on "Prediction of cognitive change based on hemispheric cortical surface maps of FDDNP." ^{18}F-FDDNP is a molecular imaging probe that binds to the neurofibrillary tangles and β-amyloid plaques. In looking at how well the distribution pattern of this tracer can predict cognitive decline, the authors examined the feasibility and reliability of using a statistical method based on ^{18}F-FDDNP PET cortical surface maps to predict a subject's Mini-Mental State Examination (MMSE) score. They found that the tracer could provide not only good visualization of brain cortical distribution of β-amyloid and neurofibrillary tangles but also reliable estimates of participants' MMSE scores (Fig. 41).

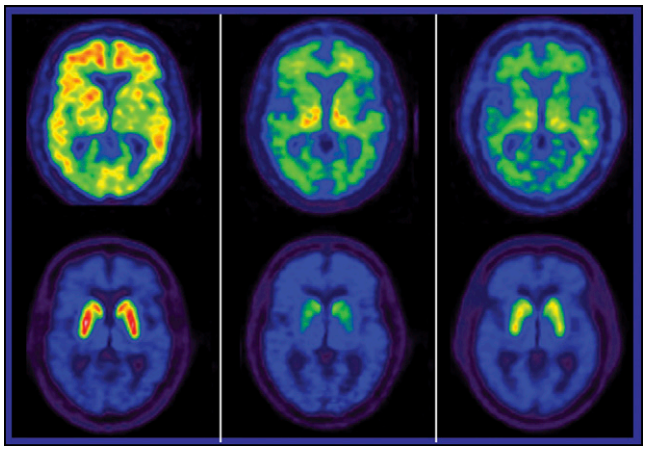

FIGURE 40. ^{11}C-PiB binding to amyloid deposition (top row) and ^{11}C-DTBZ binding to nigrostriatal dopamine projections (bottom row) in Alzheimer disease (left, with increased PiB and normal DTBA), dementia with Lewy bodies (middle, with normal PiB and greatly increased DTBZ), and frontotemporal dementia (right, with normal PiB and mildly increased DTBZ).

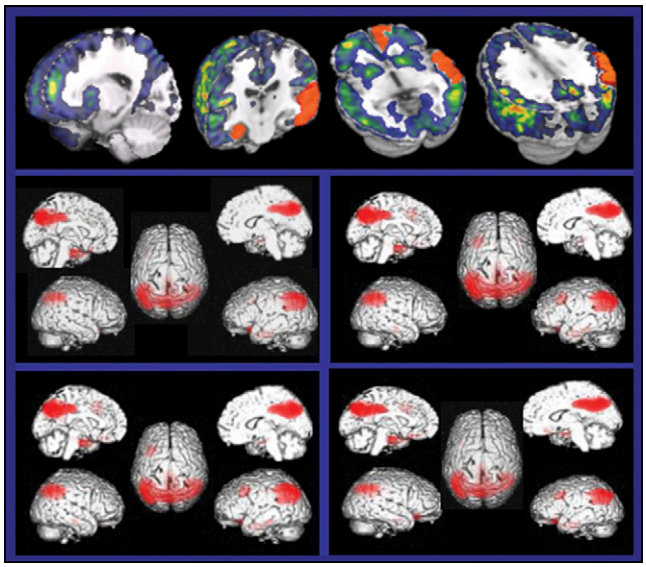

FIGURE 39. The extent and severity of abnormal ^{11}C-PiB retention on PET were correlated with hypometabolism. Top: voxel-wise Pearson product-moment correlations with parietal, precuneus, and temporal uptake (shown in remaining 4 images).

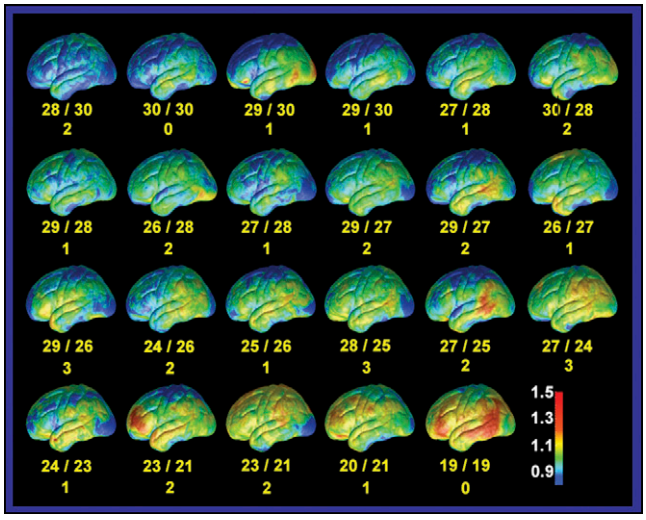

FIGURE 41. ^{18}F-FDDNP PET cortical surface maps successfully predicted participants' Mini Mental Status Examination scores.

Haense et al. [1258] from the Max Planck Institute for Neurological Research (Cologne, Germany), the University of Manchester (UK), and the Forschungszentrum Jülich (Germany) reported on "Regional cortical acetylcholine esterase activity in healthy controls, mild cognitive impairment, and Alzheimer's disease." The investigators found severe cholinergic impairment in patients with mild-to-moderate Alzheimer's disease and small but significant reductions already present in patients with mild cognitive impairment. Acetylcholine esterase reduction was most pronounced in temporal regions.

Investing in Smarter Health Care

The current administration plans to invest billions of dollars per year over the next decade in health information technology, including electronic health records and health information technologies. They expect a significant increase in about 2011 in the use of electronic health records, followed in about 2014 by a corresponding increase in data analysis. What we hear most about are the ways in which electronic health records can help in transferring data from one doctor to another or for keeping records over time. But what I would like to stress here is that these databases can be a tremendous resource for research on such things as comparative effectiveness. If created, a nationwide electronic health record system could play a major role in helping to create smarter health care. Data could be analyzed to determine the value and relative cost of molecular imaging, telling how molecular imaging can differentiate helpful and unhelpful procedures, help eliminate costly or unhelpful care, and provide more care to more people.

Quantifying Economic Value

I would suggest that some of the clinical data in studies presented at this meeting should be reanalyzed by the investigators to more precisely determine the cost effectiveness of each imaging procedure, including but not limited to its effect on prolonging survival.

Some time ago, I presented 2 equations. One shows that value is a function of knowledge; value increases as knowledge increases:

$$dV/dt = fK,$$

where V = value, K = knowledge. Knowledge improves patient care and decreases cost.

Last year I presented a model for calculating the value of a procedure:

$$V = \frac{f_5(t_5)}{f_1(t_1) + f_2(t_2) + f_3(t_3) + f_4(t_4)}$$

where t_1 = time in days from detection of disease (i.e., the onset of symptoms) until the beginning of treatment; t_2 = time in days from the beginning of treatment to the beginning of patient improvement; t_3 = total length in days of hospital stay; t_4 = time in days from onset of symptoms to time of return to normal activities; and t_5 = time from beginning of treatment to time of death. Time of survival (t_5) is not the only outcome. We can assign costs to each of these times. We can then compare results in those who undergo molecular imaging procedures with results from those who do not. The effect of the imaging procedure on these times and their costs is the index of its value. For example, we could examine the electronic health record of a patient who has undergone the imaging procedure we wish to study, recording times t_1–t_5. We would then compare these times with those in similar patients who did not undergo the imaging procedure, converting time in days to cost.

Decades ago, we examined hospital records of 1,000 patients with brain tumors who had been seen at Johns Hopkins before 1960. None had undergone brain scans. We compared the time between the onset of symptoms and the time of surgery in this group and in another group of 1,000 patients cared for after 1960. All of the later group had undergone rectilinear brain scans. The time between onset of symptoms and surgery fell by 50% in the later set of patients. The scan increased the certainty that the patient indeed had a brain tumor. However, comparison of the 2 groups indicated no increase in survival time after surgery. The neurosurgeons told me at the time that they were not surprised at this finding, because the effects of surgery compounded the effects of the tumor.

In the future, databases will encode the results of all patient-specific clinical, laboratory, and imaging studies. This is feasible today. For example, Google can scan 6 billion sites in 90 languages for 138,000 persons every minute. The Defense Department and the Department of Veterans Affairs are building an electronic database of administrative and medical information for U.S. service personnel. A new Joint Virtual Lifetime Record will track individuals once they enlist, through their military service and beyond. This electronic health system will help deliver health care benefits to veterans and active-duty military members and serve as a model for the rest of the United States.

The question arises as to whether prior approval will be needed for all imaging studies in the future. Many insurers today, including Aetna, Inc., WellPoint, Inc., and CIGNA Corporation, have radiology benefits managers. A doctor caring for a patient must get permission before the insurer will agree to pay for an imaging procedure. Their goal is to ensure that doctors use high-tech imaging only when the administrators agree that the patient having the studies will benefit. William Donaldson, former chair of the U.S. Securities and Exchange Commission, said, "There is a limit to how much regulation can do. In the final analysis, you could write all the rules you want, but there has to be a philosophy of ethical behavior that comes from human beings operating in a professional way."

Summary

This excellent meeting has illustrated in many different ways the key point that molecular processes are the key to health. These processes move down below the cellular level. Although we still operate with approaches based on the cellular level of disease, we are now capable of understanding the molecular processes. Molecular medicine is the key to "smarter health care." The patients' and physicians' brains will remain the most important computers in health care. But in the future, every nuclear imaging physician will have video connectivity with the patient, consultants, and computer access to databases of medical knowledge. The benefits of the few must be made the benefits of all.

Henry N. Wagner, Jr., MD
Johns Hopkins University Hospital Baltimore, MD